Theor Chem Acc (2011) 128:183–189
DOI 10.1007/s00214-010-0813-8

REGULAR ARTICLE

Dual-level direct dynamics studies on the hydrogen abstraction reactions of fluorine atoms with CF_3CH_2X(X=F, Cl)

Li Wang · Yuan Zhao · Jing Zhang · Yanna Dai · Jinglai Zhang

Received: 14 April 2010 / Accepted: 31 August 2010 / Published online: 14 September 2010

Abstract The kinetic properties of the hydrogen abstraction reactions of $CF_3CH_2F + F \rightarrow CF_3CHF + HF$ (R1) and $CF_3CH_2Cl + F \rightarrow CF_3CHCl + HF$ (R2) have been studied by dual-level direct dynamics method. Optimized geometries and frequencies of all the stationary points and extra points along the minimum-energy path (MEP) were obtained at the B3LYP/6-311 + G(2d,2p) level. Two complexes with energies less than that of the reactants were located in the reactant side of each reaction. The energy profiles were further refined with the interpolated single-point energies (ISPE) method at the G3(MP2) level of theory. Using canonical variational transition state theory (CVT) with the small-curvature tunneling correction (SCT) method, the rate constants were evaluated over a wide temperature range of 200–2,000 K. Our calculations have shown that C–H bond activity decreases when one hydrogen atom of CF_3CH_3 is substituted by a fluorine atom, than when substituted with a chlorine atom. This is in good agreement with the experimental results.

Keywords DFT · Rate constants · Direct dynamics method

Electronic supplementary material The online version of this article (doi:10.1007/s00214-010-0813-8) contains supplementary material, which is available to authorized users.

L. Wang · Y. Zhao · Jing Zhang · Y. Dai · Jinglai Zhang (✉)
Institute of Environmental and Analytical Sciences,
Institute of Fine Chemistry and Engineering,
College of Chemistry and Chemical Engineering,
Henan University, Kaifeng, Henan 475004,
People's Republic of China
e-mail: zhangjinglai@henu.edu.cn

1 Introduction

Chlorofluorocarbons (CFCs) contribute to two very important global ecological consequences with their emission into the atmosphere. One is that the photolysis of CFCs by ultraviolet solar radiation produces chlorine atoms that can initiate the chain destruction of ozone. The other is that CFCs contribute to greenhouse effect by absorbing the earth's infrared emission. Considering the adverse effects of CFCs, an international effort has been made to replace CFCs with environmentally friendly alternatives. Hydrofluorocarbons (HFCs) and hydrochlorofluorocarbons (HCFCs) are considered to be two important classes of CFCs substitutes used in refrigeration, foam blowing and cleaning applications. Moreover, the inclusion of at least one C–H bond makes them react readily with OH radicals, oxygen atoms, and other atmospheric constituents. Here, we focus our attention on the reactions of HFC-134a (CF_3CH_2F) and HCFC-133a (CF_3CH_2Cl) with fluorine atoms. HFC-134a (CF_3CH_2F), the principal CFCs alternative, has been used in air-conditioning applications and new model automobiles [1–3]. As to HCFC-133a (CF_3CH_2Cl), it has not been applied in large scale of industrial applications although its structure is similar to HFC-134a. However, its kinetic parameters have also been studied here for comparison with HFC-134a. Owing to their importance, numerous experimental and theoretical studies have been performed for the reactions of HCFCs with OH radicals and Cl atoms [1, 4–12]. On the contrary, limited experimental data are available for the reactions of F atoms with CF_3CH_2F and CF_3CH_2Cl, especially for the temperature dependence of rate constants [12–16]. The reactions of HFC-134a and HCFC-133a with fluorine atoms deserve our attention because fluorine atoms can react with most trace atmospheric compounds rapidly. In the early literature,

the rate constants of $CF_3CH_2F + F \rightarrow CF_3CHF + HF$ (R1) were measured around room temperature, and in the temperature ranges of 210–363 K [14] and 296–381 K [12], and they did not show significant discrepancies. The corresponding Arrhenius expressions (in cm^3 $molecule^{-1}$ s^{-1}) $(9.8^{+9}_{-5}) \times 10^{-11} \exp[-(1{,}130 \pm 190)/T]$ (210–363 K) and $(6.5^{+2.1}_{-1.6}) \times 10^{-11} \exp[-(1{,}100 \pm 100)/T]$ (296–381 K) were obtained by Maricq et al. [14] and Louis et al. [12], respectively. Although these two expressions exhibit good consistency, both expressions have large uncertainties. On the other hand, the rate constant of $CF_3CH_2Cl + F \rightarrow CF_3CHCl + HF$ (R2) has only been measured at 296 K ($(2.1 \pm 0.5) \times 10^{-12}$ cm^3 $molecule^{-1}$ s^{-1}) by Møgelberg et al. [16].

As for theoretical studies, Louis et al. [12] have calculated the rate constant of reaction R1 at room temperature. However, only one-dimensional tunneling was considered, and they did not calculate the rate constants at other temperatures. In the available experimental and theoretical studies in rate constants determination, the temperatures used are still far from covering the whole temperature range of practical interest. Thus, the accurate extrapolation of rate constants to higher temperatures requires theoretical studies.

In this work, we employed dual-level (X//Y) [17–19] direct dynamic method to study the kinetic nature of both reactions over a wide temperature range. In this methodology, the potential energy information can be calculated directly from a sufficiently accurate molecular orbital (MO) theory only in the region of configuration space along a reaction path, without the intermediary of a potential surface fit. As usual, dual-level X//Y refers to optimization and frequencies at lower-level Y with single-point energies calculated at higher-level X. Here, the electronic structure information is obtained directly from density functional theory (DFT) calculations. Then, single-point energies were calculated by G3(MP2) method based on the lower level DFT geometries. Subsequently, by means of the Polyrate 9.7 program [20], the rate constants were calculated using the variational transition-state theory (VTST) [21–23], proposed by Truhlar and coworkers. The comparison between theoretical and experimental results will be discussed.

The knowledge of the standard enthalpy of formation of the species is important in evaluating feasible reaction pathways and stability of intermediates. However, the enthalpies of formation of species CF_3CH_2Cl and CF_3CHCl have not been determined experimentally. We attempt to estimate their enthalpies of formation using ab initio and DFT methods by two sets of isodesmic reactions.

2 Computational methods

The geometries of the stationary points (reactants, products, complexes, and transition states) were calculated with Becke's three-parameter nonlocal-exchange functional with the nonlocal correlation functional of Lee–Yang–Parr [24, 25] with 6-311 + G(2d,2p) basis set (B3LYP/6-311 + G(2d,2p)). To obtain more reliable reaction enthalpies and barrier heights, high-level single-point calculations for the stationary points were performed by G3(MP2) [26] theory based on the B3LYP-optimized geometries. Reactants and products were characterized by frequency calculations and have positive definite Hessian matrices. Transition states (TSs) showed only one negative eigenvalue in their diagonalized force constant matrices, and their associated eigenvectors were confirmed to correspond to the motion along the reaction coordinate under consideration, using the intrinsic reaction coordinate (IRC) method. The first and second energy derivatives at geometries along the MEP were obtained to calculate the curvature of the reaction path and the generalized vibrational frequencies along the reaction path. The dual-level potential profile along the reaction path was further refined with the interpolated single-point energies (ISPE) method [27], in which a few extra single-point calculations were needed to correct the lower level reaction path. All the electronic structure calculations were performed by the Gaussian 03 program package [28].

To estimate the enthalpies of formation (ΔH^0_{f298}) of the species CF_3CH_2Cl and CF_3CHCl, two sets of isodesmic reactions were employed.

For CF_3CH_2Cl,

$$CF_3CH_2Cl + CH_4 \rightarrow CH_3CH_2Cl + CHF_3 \quad \text{(R3)}$$

$$CF_3CH_2Cl + C_2H_6 \rightarrow CH_3CH_2Cl + CF_3CH_3 \quad \text{(R4)}$$

For CF_3CHCl,

$$CF_3CHCl + CH_4 \rightarrow CF_3CH_2Cl + CH_3 \quad \text{(R5)}$$

$$CF_3CHCl + C_2H_6 \rightarrow CF_3CH_2Cl + C_2H_5 \quad \text{(R6)}$$

The evaluated enthalpies of formation for the four reactions are the unweighted average of the results obtained by the G3(MP2)//B3LYP/6-311 + G(2d,2p) and G3(MP2)//MP2/6-311 + G(2d,2p) levels in this study.

The rate constants were calculated by using the variational transition state theory (VTST) proposed by Truhlar and coworkers. The specific level of VTST that we have used is the canonical variational transition-state theory (CVT) [29–31] with the small-curvature tunneling (SCT) [32, 33] method. The canonical variational transition state theory rate constant, $k^{CVT}(T)$, at fixed temperature (T) by minimizing generalized transition state theory rate

constant, $k^{GT}(T,s)$, with respect to the dividing surface at s is expressed as

$$k^{CVT}(T) = \min_{s} k^{GT}(T,s)$$

The generalized transition state theory rate constant, k^{GT}, for temperature T and dividing surface at s is

$$k^{GT}(T,s) = \frac{\sigma Q^{GT}(T,s)}{\beta h Q^{R}(T)} \exp(-\beta V_{MEP}(s))$$

In this equation, s is the location of the generalized transition state on the IRC; σ is the symmetry factor accounting for the possibility of two or more symmetry-related reaction paths; β equals $(k_B\ T)^{-1}$ where k_B is Boltzmann's constant, h is Plank's constant; $Q^{R}(T)$ is the reactant's partition function per unit volume, excluding symmetry numbers for rotation; $V_{MEP}(s)$ is the classical energy along the MEP overall zero of energy at the reactant. $Q^{GT}(T, s)$ is the partition function of the generalized transition state at s along the MEP. To include tunneling effect, the CVT rate constant is multiplied by the small-curvature tunneling (SCT) approximation, which is denoted as $k^{CVT/SCT}(T)$. Note that the $^2P_{1/2}$ and $^2P_{3/2}$ electronic states of the fluorine atom, with a 404 cm^{-1} splitting due to the spin–orbit coupling, are used in the calculation of the electronic partition functions. The curvature components were calculated by using a quadratic fit to obtain the derivative of the gradient with respect to the reaction coordinate. The rate constants calculations were performed by the POLYRATE 9.7 program.

3 Results and discussion

3.1 Stationary points

The geometric parameters of all of the reactants, products, complexes, and transition states optimized at the B3LYP/6-311 + G(2d,2p) level, as well as available experimental and theoretical results calculated at the MP2/6-31G(d,p) level [12], are shown in Fig. 1. It can be seen that the calculated H–F bond length (0.92 Å) is the same as the corresponding experimental value (0.92 Å) [34]. The results obtained at the B3LYP/6-311 + G(2d,2p) level agree well with those obtained at the MP2/6-31G(d,p) level [12] with relative error of 9%, except for the bond length between F and H in TS1. The breaking C–H bonds are stretched by 0.28 and 1.57% in transition states of TS1 and TS2, respectively, with respect to the C–H equilibrium bond lengths in CF_3CH_2F and CF_3CH_2Cl. The forming H–F bonds are elongated by 149.7 and 97.4% with respect to the equilibrium bond lengths in isolated HF molecule, respectively. The two transition states resemble the reactants more than the products, i.e., both reactions proceed via ''early'' transition states.

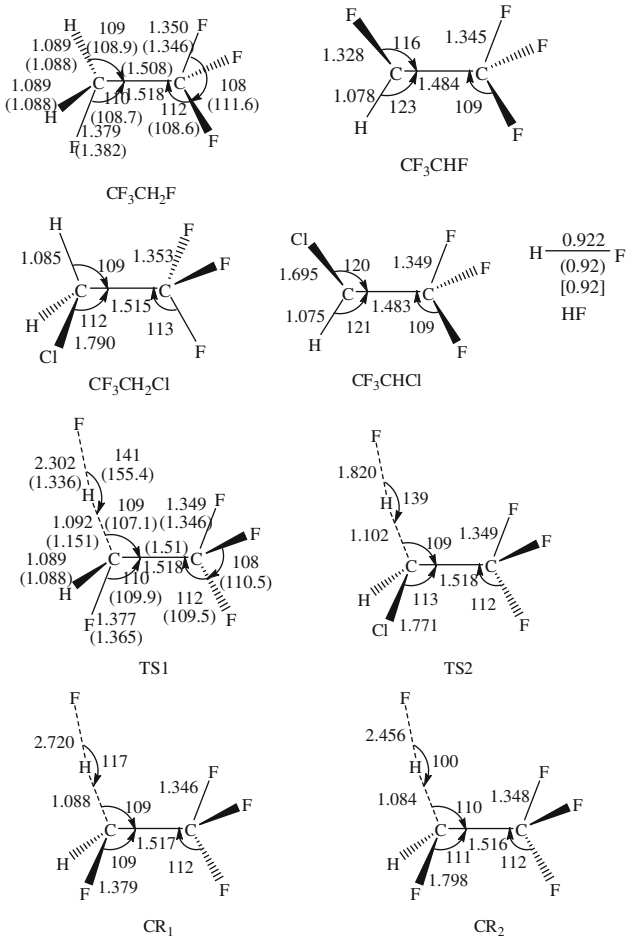

Fig. 1 Optimized geometries of reactants, products, complexes, and saddle points at the B3LYP/6-311 + G(2d,2p) leve1. The value in the *square bracket* is experimental value [34]. The values in the *parentheses* are the theoretical values obtained at the MP2/6-31G(d,p) [12]. Bond lengths are in angstroms and angles are in degrees

The harmonic vibrational frequencies of the reactants, products, complexes, and transition states calculated at the B3LYP/6-311 + G(2d,2p) level, as well as the available experimental and theoretical values are listed in Table 1. The frequency of HF obtained at the B3LYP/6-311 + G(2d,2p) level reproduces experimental [35] and theoretical value [12] relatively well, with deviation of 1% and 2%, respectively. However, the frequencies of CF_3CH_2F, CF_3CHF, and TS1 calculated at the B3LYP/6-311 + G(2d,2p) and MP2/6-31G(d,p) levels have large deviation, especially for small frequencies. The reactants and products have all real frequencies, and transition states were confirmed to have only one negative eigenvalue in their diagonalized force constant matrices.

Table 1 Calculated Frequencies (in cm^{-1}) of the reactants, products, complexes, and saddle points at the B3LYP/6-311 + G(2d,2p) leve1, experimental result for HF in the parentheses and theoretical values at the MP2/6-31G(d,p) level

Species	B3LYP/6-311 + G(2d, 2p)	MP2/6-31G(d,p)
HF	4,097 (4,138[a])	4,192[b]
CF_3CH_2F	107, 216, 346, 403, 522, 538, 653, 833, 966, 1,089, 1,144, 1,180, 1,285, 1,300, 1,433, 1,491, 3,080, 3,138	114, 216, 358, 412, 530, 549, 668, 865, 1,021, 1,147, 1,246, 1,247, 1,360, 1,363, 1,508, 1,563, 3,170, 3,245[b]
CF_3CH_2Cl	96, 182, 347, 349, 523, 525, 627, 782, 843, 905, 1,100, 1,119, 1,260, 1,282, 1,340, 1,472, 3,115, 3,178	
CF_3CHF	78, 210, 301, 412, 443, 544, 570, 668, 854, 1,080, 1,150, 1,189, 1,261, 1,432, 3,238	86, 213, 352, 419, 517, 556, 673, 724, 884, 1,211, 1,229, 1,254, 1,340, 1,505, 3,325[b]
CF_3CHCl	34, 182, 214, 363, 401, 528, 557, 644, 817, 932, 1,086, 1,119, 1,230, 1,349, 3,256	
CR1	25, 62, 99, 114, 217, 348, 405, 522, 540, 652, 829, 960, 1,088, 1,146, 1,172, 1,277, 1,299, 1,435, 1,491, 3,082, 3,142	
CR2	7, 74, 121, 171, 302, 346, 350, 523, 525, 628, 764, 842, 905, 1,094, 1,132, 1,247, 1,274, 1,333, 1,467, 3,124, 3,194	
TS1	199i, 19, 25, 97, 216, 333, 403, 521, 537, 652, 832, 961, 1,079, 1,146, 1,161, 1,261, 1,292, 1,427, 1,476, 2,946, 3,113	1,479i, 21, 73, 110, 217, 316, 406, 521, 544, 667, 715, 867, 979, 1,184, 1,257, 1,267, 1,345, 1,413, 1,447, 1,641, 3,219[b]
TS2	414i, 42, 77, 102, 180, 335, 350, 524, 527, 621, 754, 824, 894, 1,061, 1,127, 1,229, 1,263, 1,312, 1,413, 2,656, 3,146	

[a] Ref. [35]

[b] Ref. [12]

Due to the lack of experimental heats of formation for the CF_3CH_2Cl and CF_3CHCl species, it is difficult to compare calculated reaction enthalpies with experimental data. Here, enthalpies of formation of the above two species were estimated by four isodesmic reactions (R3–R6). The reaction enthalpies of R3–R6 were first calculated, and these theoretical results combined with the known enthalpies of formation (CH_4, -17.88 kcal mol^{-1}; C_2H_6, -20.0 kcal mol^{-1}; CH_3CH_2Cl, -26.8 kcal mol^{-1}; CHF_3, -166.8 kcal mol^{-1}; CF_3CH_3, -179 ± 2 kcal mol^{-1}; CH_3, 35 ± 0.2 kcal mol^{-1}; C_2H_5, 28.4 ± 0.5 kcal mol^{-1}) [36] to estimate the required enthalpies of formation of target species at 298 K. The ΔH^0_{f298} calculated at the G3(MP2)//B3LYP/6-311 + G(2d,2p) and G3(MP2)//MP2/6-311 + G(2d,2p) levels is presented in Table 2. Note that the error limits are calculated by adding the maximum uncertainties of ΔH^0_{f298} values of the reference compounds taken from the literature. The enthalpies of formation are -179.76 ± 2.0 kcal mol^{-1} for CF_3CH_2Cl and -131.93 ± 4.7 kcal mol^{-1} for CF_3CHCl. The calculated results based on two sets of isodesmic reaction show good consistency at two levels.

The reaction enthalpies (ΔH^0_{298}) and barrier heights (ΔE(0 K)) of reactions R1 and R2 calculated at the B3LYP/6-311 + G(2d,2p) and G3(MP2)//B3LYP/6-311 + G(2d,2p) levels as well as the available experimental result are summarized in Table 3. The calculated reaction enthalpy of -34.16 kcal mol^{-1} for reaction R1 at higher level agrees well with the corresponding experimental value of -33.14 ± 3.3 kcal mol^{-1}, which is derived from the experimental heats of formation (CF_3CH_2F, -214 ± 1 kcal mol^{-1}; CF_3CHF, -163 ± 2 kcal mol^{-1}; F, 19.0 ± 0.1 kcal mol^{-1}; HF, -65.14 ± 0.2 kcal mol^{-1}) [36]. Our calculated value also shows good consistency with the value of -33.49 kcal mol^{-1}, which was calculated at the PMP2/6-311G(2d,2p)//MP2/6-31G(d,p) level by Louis et al. [12]. It can be inferred that the reaction enthalpy of R2 calculated at the same level is credible although no experimental value is available for comparison. For both reactions, the complexes located at the entrance with the

Table 2 Calculated enthalpies of formation at 298 K (in kcal mol^{-1})

	G3(MP2)//B3LYP/6-311 + G(2d,2p)	G3(MP2)//MP2/6-311 + G(2d,2p)	Average value and deviation
$CF_3CH_2Cl + CH_4$	-180.47	-180.47	-179.76 ± 2.0
$CF_3CH_2Cl + C_2H_6$	-179.10 ± 2.0	-179.00 ± 2.0	
$CF_3CHCl + CH_4$	-131.39 ± 2.2	-131.28 ± 2.2	-131.93 ± 4.7
$CF_3CHCl + C_2H_6$	-132.51 ± 2.5	-132.55 ± 2.5	

Table 3 Enthalpies (in kcal mol^{-1}) and barrier heights (in kcal mol^{-1}) at B3LYP/6-311 + G(2d,2p) and G3(MP2)//B3LYP/6-311 + G(2d,2p) levels and available experimental value

	$CF_3CH_2F + F$		$CF_3CH_2Cl + F$	
	ΔH^0_{298}	ΔE(0 K)	ΔH^0_{298}	ΔE(0 K)
B3LYP/6-311 + G(2d,2p)	−35.02	−0.63	−37.63	−2.80
G3(MP2)//B3LYP/6-311 + G(2d,2p)	−34.16	−1.20	−36.77	1.15
Expt.[a]	−33.14 ± 3.3			

[a] Ref. [36]

relative energies of 1.43(CR_1) and 2.25(CR_2) kcal mol^{-1} lower than the reactants at the G3(MP2)//B3LYP level are first formed. From the complex, the reaction passes through a transition state to form the products. The barrier heights calculated at the B3LYP/6-311 + G(2d,2p) level are −0.60 kcal mol^{-1} for R1 and −2.80 kcal mol^{-1} for R2. The corresponding values are −1.20 and 1.15 kcal mol^{-1} at the G3(MP2)//B3LYP/6-311 + G(2d,2p) level, respectively.

The MEP for each reaction was obtained by the intrinsic reaction coordinate (IRC) theory at the B3LYP6-311 + G(2d,2p) level, and the kinetics calculations of the title reactions were carried out with the VTST-ISPE method at the G3(MP2)//B3LYP level. The classical potential energy ($V_{MEP}(s)$), the ground-state vibrational adiabatic potential energy ($V_a^G(s)$), and the zero-point energy (ZPE) curves of reaction R1 as functions of the intrinsic reaction coordinate (s) are plotted in Fig. 2, where $V_a^G(s) = V_{MEP}(s) + ZPE(s)$. It should be noted that the locations of maxima on the $V_a^G(s)$ and $V_{MEP}(s)$ energy curves shift in the s direction toward the products, and the maxima of the curves are slightly higher than the reactants. This is the case when the saddle-point position of the dual level is generally shifted. The same conclusion can be drawn from the other reaction.

3.2 Kinetics calculation

Dual-level (X//Y) direct dynamics calculations were carried out for both reactions using the variational transition-state theory. The PES information for each reaction obtained at the G3(MP2)//B3LYP/6-311 + G(2d,2p) level is put into Polyrate 9.7 program to calculate the VTST rate constants over a temperature range of 200–2,000 K. The forward rate constants were calculated by canonical variational transition-state theory (CVT) with the small-curvature tunneling (SCT) method. The TST, CVT, CVT/SCT, and available experimental rate constants for both reactions in the temperature range of 200–2,000 K are presented in Table S and Fig. 3a, b. As shown in Fig. 3a, the calculated rate constants of reaction R1 are in good

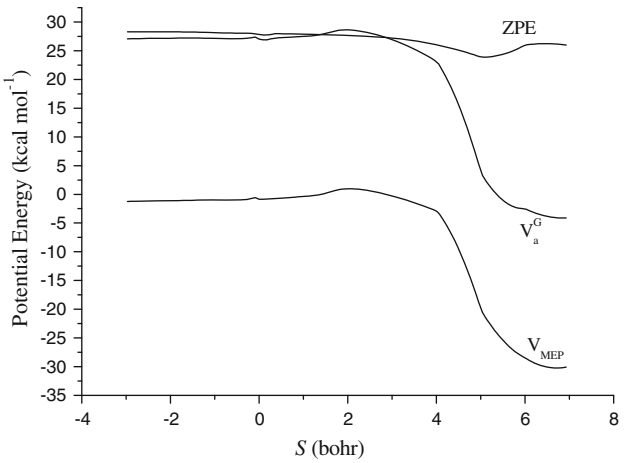

Fig. 2 Classical potential energy curve (V_{MEP}), ground-state vibrationally adiabatic energy curve (V_a^G), and zero-point-energy curve ZPE as functions of s bohr at the G3(MP2)//B3LYP/6-311 + G(2d,2p) level for $CF_3CH_2F + F \rightarrow CF_3CHF + HF$

agreement with most of experimental values with deviation within a factor of 0.74–1.53, except for the experimental result at 363 K reported by Maricq et al. (5.90×10^{-12} $cm^3 molecule^{-1} s^{-1}$). This value is also higher than other experimental values. The calculated activation energies 1.02 and 0.86 kcal mol^{-1} are slightly lower than corresponding experimental values of 2.19 ± 0.2 [14] and 2.25 ± 0.4 [12] kcal mol^{-1} in the temperature ranges of 296–381 and 210–363 K, respectively. However, both experimental values also have big uncertainties, especially for the preexponent that is almost doubled. After considering the error limits of experiments, there is good consistency between calculated and experimental results. For the other reaction $CF_3CH_2Cl + F \rightarrow CF_3CHCl + HF$ (R2), the calculated result is in a good accord with the only available experimental value at 296 K.

The CVT/SCT rate constants of reaction R2 are greater than those of reaction R1 below 500 K. The Arrhenius expressions ($k = Aexp(-E_a/RT)$) are fitted based on the calculated CVT/SCT rate constants in the temperature range of 200–500 K. Plot of the $\ln k_{CVT/SCT}$, calculated at the G3(MP2)//B3LYP/6-311 + G(2d,2p) level, versus 1/T, which is between 200 and 500 K, is almost a straight line. The slope and intercept are obtained, and finally the pre-exponential factor (A) and activation energies (E_a) are calculated through intercept and slope of the straight line. The corresponding values are summarized in the Table 4. After the chlorine atom of CF_3CH_2Cl is substituted by fluorine atom, the A of reaction R1 (7.58×10^{-12}) is much smaller than that of reaction R2 (1.76×10^{-11}), whereas the calculated activation energies are very close (0.90 vs. 1.09 kcal mol^{-1}) to each other. Thus, the rate constants of R2 are little larger than those of R1. This conclusion can

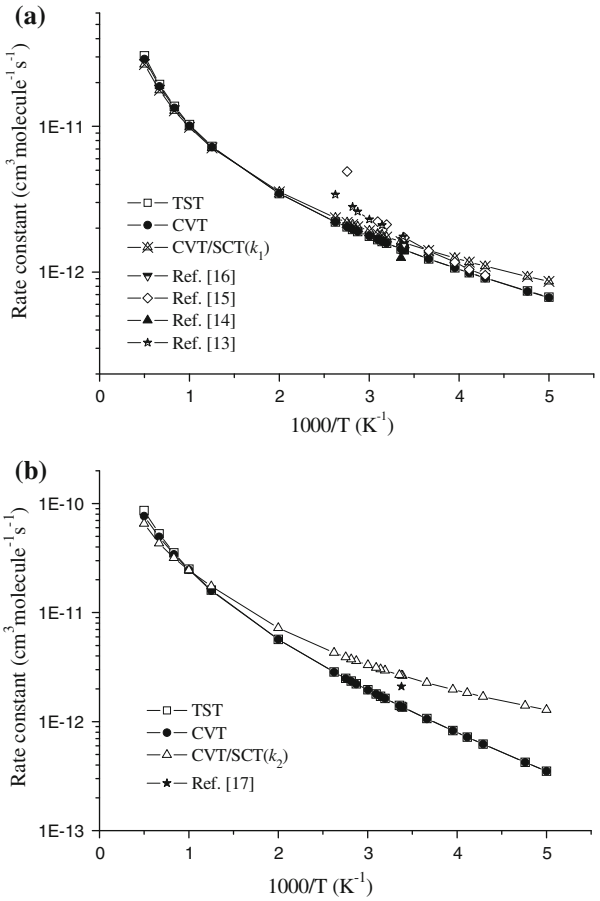

Fig. 3 **a** Plot of the TST, CVT, and CVT/SCT rate constants calculated at the G3(MP2)//B3LYP/6-311 + G(2d,2p) level and the available experimental values versus 1,000/T between 200 and 2,000 K for the $CF_3CH_2F + F \rightarrow CF_3CHF + HF$. **b** Plot of the TST, CVT, and CVT/SCT rate constants calculated at the G3(MP2)//B3LYP/6-311 + G(2d,2p) level and the available experimental values versus 1,000/T between 200 and 2,000 K for the $CF_3CH_2Cl + F \rightarrow CF_3CHCl + HF$

also be justified by the C–H bond dissociation energies. The C–H bond dissociation energies are 102.12 and 99.51 kcal mol^{-1} for CF_3CH_2F and CF_3CH_2Cl at the G3(MP2)//B3LYP/6-311 + G(2d,2p) level, respectively. Our calculation indicates that fluorine substitution deactivates the C–H bond compared with chlorine substitution.

It can also be reflected from Fig. 3a that for the reaction $CF_3CH_2F + F \rightarrow CF_3CHF + HF$ (R1), the rate constants of TST and CVT are nearly the same over a whole temperature range, which means that the variational effect for reaction R1 is almost negligible. While the CVT/SCT rate constants are larger than the CVT ones at lower temperatures, the ratios of $k_{CVT/SCT}/k_{CVT}$ are in the range of 1.03–1.29. Thus, small-curvature tunneling (SCT) effect on the rate constants is small for reaction R1. A similar conclusion can be made for the reaction R2. For a typical reaction $A + BC \rightarrow AB + C$, the skewed angle θ of the reaction path curvature is defined by the expression $\cos\theta = \sqrt{m_A m_C/(m_A + m_B)(m_C + m_B)}$. For these two reactions, the θ values are 14.1° for R1 and 13.9° for R2, which indicate that the large curvature tunneling (LCT) may have some influence on the rate constants calculations. Moreover, since the H-abstraction of the title reaction is between two heavy fragments, the LCT correction would be desirable. However, the LCT correction cannot be directly calculated by means of the ab initio or DFT potential energy surface. The LCT effect can only be made when the analytic representation of the potential energy surface is available, which is beyond the capabilities of our computational resources. Considering that the skewed angle θ is almost the same for the two reactions, the inclusion of the LCT correction may not change the qualitative results. Our calculated rate constants with SCT correction show good agreement with the experimental values. In addition, the SCT correction has been applied widely to evaluate the rate constants in the heavy-light-heavy mass combination for the hydrogen abstraction reactions, in which the skewed angle θ is almost the same or smaller than those of reactions R1 and R2 [37–41]. So it is reasonable to believe that rate constants including the SCT correction are reliable.

Table 4 Arrhenius parameters for the title reactions

	A (cm^3 s^{-1})	E_a (kcal mol^{-1})
$CF_3CH_2F + F$	7.58×10^{-12}	0.90
$CF_3CH_2Cl + F$	1.76×10^{-11}	1.09

In temperature range of 200−500 K

Owing to the good agreement between the theoretical and experimental values, it is reasonable to believe that the present calculations can provide reliable predictions for the rate constants of the title reactions at higher temperatures. This will be useful for atmospheric modeling calculations that can help to assess the atmospheric lifetimes of HCFCs. Therefore, for the convenience of future experimental measurements, the theoretical rate constants of title reactions within 200–2,000 K are fitted by the following expressions (in cm^3 molecule^{-1} s^{-1}): $k_1 = 6.0 \times 10^{-16} T^{1.41} \exp(-41.3/T)$ and $k_2 = 7.0 \times 10^{-16} T^{1.52} \exp(-121.1/T)$.

4 Conclusions

In this paper, the hydrogen abstraction reactions of CF_3CH_2X(X = F, Cl) with F atoms were investigated by dual-level direct dynamic method. The average values of heats of formation for CF_3CH_2Cl and CF_3CHCl are −179.76 ± 2.0 and −131.93 ± 4.7 kcal mol^{-1}, respectively, using ab initio and density functional calculations

via two sets of isodesmic reactions. The rate constants calculated by the variational transition-state theory (VTST) at the G3(MP2)//B3LYP/6-311 + G(2d,2p) level are observed to mutually agree well with the available experimental values. The rate constants of R2 are greater than those of R1, which is the opposite direction of C–H bond dissociation energies. The chlorine substitution increases the reactivity of C–H bond compared with the fluorine substitution in CF_3CH_3. The three-parameter expressions (in cm^3 $molecule^{-1}$ s^{-1}) for both reactions over the whole temperatures are $k_1 = 6.01 \times 10^{-16}\ T^{1.41}\ \exp(-41.3/T)$ and $k_2 = 7.0 \times 10^{-16}\ T^{1.52}\ \exp(-121.1/T)$, respectively.

Acknowledgments We thank Professor Donald G. Truhlar for providing of the POLYRATE 9.7 program. This work was supported by the National Natural Science Foundation of China (21003036), the Science Foundation of Henan Province (2008A150005), Science Foundation of Henan University (2009YBZR013, SBGJ090507), Doctor Foundation of Henan University.

References

1. Orkin VL, Khamaganov VG (1993) J Atmos Chem 16:157
2. Montzka SA, Myers RC, Butler JM, Elkins JW, Lock LT, Clarke AD (1996) Geophys Res Lett 23:169
3. Franklin J (1993) Chemosphere 27:1565
4. Bednarek G, Breil M, Hoffmann A, Kohlmann JP, Mors V, Zellner R (1996) Ber Bunsenges Phys Chem 100:528
5. Urata S, Takada A, Uchimaru T, Chandra AK (2003) Chem Phys Lett 368:215
6. Cohen N, Benson SW (1987) J Phys Chem 91:162
7. Fang TD, Taylor PH, Berry RJ (1999) J Phys Chem A 103:2700
8. Chiorboli C, Piazza R, Tosato ML, Carassiti V (1993) Coord Chem Rev 125:241
9. Gierczak T, Talukdar R, Vaghjiani GL, Lovejoy ER, Ravishankara AR (1991) J Geophys Res 96:5001
10. Sawerysyn JP, Talhaoui A, Meriaux B, Devolder P (1992) Chem Phys Lett 198:197
11. Tuazon EC, Atkinson R, Corchnoy SB (1992) Int J Chem Kinet 24:639
12. Louis F, Talhaoui A, Sawerysyn J-P, Rayez M-T, Rayez J-C (1997) J Phys Chem A 101:8503
13. Moore C, Smith IWM (1995) J Chem Soc Faraday Trans 91:3041
14. Maricq MM, Szente JJ, Hurley MD, Wallington TJ (1994) J Phys Chem 98:8962
15. Wallington TJ, Hurley MD, Shi J, Maricq MM, Sehested J, Nielsen OJ, Ellermann T (1993) Int J Chem Kinet 25:651
16. Møgelberg TE, Nielsen OJ, Sehested J, Wallington TJ (1995) J Phys Chem 99:13437
17. Truhlar DG (1995) In: Heidrich D (ed) The reaction path in chemistry: current approaches and perspectives. Kluwer, Dordrecht, p 229
18. Truhlar DG, Garrent BC, Klippenstein SJ (1996) J Phys Chem 100:12771
19. Hu WP, Truhlar DG (1996) J Am Chem Soc 118:860
20. Corchado JC, Chuang YY, Past PL, Hu WP, Liu YP, Lynch GC, Nguyen KA, Jackels CF, Fernandez-Ramos A, Ellingson BA, Lynch BJ, Zheng JJ, Melissas VS, Villa J, Rossi I, Coitino EL, Pu JZ, Albu TV, Steckler R, Garrett BC, Isaacson AD, Truhlar DG (2007) POLYRATE, version 9.7. University of Minnesota, Minneapolis
21. Truhlar DG, Garrett BC (1980) Acc Chem Res 13:440
22. Truhlar DG, Isaacson AD, Garrett BC (1985) In: Baer M (ed) The theory of chemical reaction dynamics. CRC Press, Boca Raton, p 65
23. Truhlar DG, Garrett BC (1984) Annu Rev Phys Chem 35:159
24. Becke AD (1993) J Chem Phys 98:1372
25. Lee C, Yang W, Parr RG (1998) Phys Rev B 37:785
26. Curtiss LA, Redfem PC, Raghavachari K, Rassolov V, Pople JA (1999) J Chem Phys 110:4703
27. Chuang YY, Corchado JC, Truhlar DG (1999) J Phys Chem 103:1140
28. Frisch MJ, Truck GW, Schlegel HB, Scuseria GE, Robb MA, Cheeseman JR, Zakrzewski VG, Montgomery JA, Stratmann RE Jr, Burant JC, Dapprich S, Millam JM, Daniels AD, Kudin KN, Strain MC, Farkas O, Tomasi J, Barone V, Cossi M, Cammi R, Mennucci B, Pomelli C, Adamo C, Clifford S, Ochterski J, Petersson GA, Ayala PY, Cui Q, Morokuma K, Malick DK, Rabuck AD, Raghavachari K, Foresman JB, Cioslowski J, Ortiz JV, Boboul AG, Stefnov BB, Liu G, Liaschenko A, Piskorz P, Komaromi L, Gomperts R, Martin RL, Fox DJ, Keith T, Al-Laham MA, Peng CY, Nanayakkara A, Gonzalez C, Challacombe M, Gill PMW, Johnson B, Chen W, Wong MW, Andres JL, Gonzalez C, Head-Gordon M, Replogle ES, Pople JA (2003) GAUSSIAN 03, Revision A.1, Guassian Inc., Pittsburgh
29. Garrett BC, Truhlar DG (1979) J Chem Phys 70:1593
30. Garrett BC, Truhlar DG (1979) J Am Chem Soc 101:4534
31. Garrett BC, Truhlar DG, Grev RS, Magnuson AW (1980) J Phys Chem 84:1730
32. Lu DH, Truong TN, Melissas VS, Lynch GC, Liu YP, Garrett BC, Steckler R, Issacson AD, Rai SN, Hancock GC, Lauderdale JG, Joseph T, Truhlar DG (1992) Comput Phys Commun 71:235
33. Liu Y-P, Lynch GC, Truong TN, Lu D-H, Truhlar DG, Garrett BC (1993) J Am Chem Soc 115:2408
34. Mason MG, Von Holle WG, Robinson DW (1971) J Chem Phys 54:3491
35. Webb DU, Rao KN (1968) J Mol Spectrosc 28:129
36. DeMore WB, Sander SP, Golden SP, Howard CJ, Golden DM, Kolb CE, Hampson RF, Molina MJ (1997) Chemical kinetics and photochemical data for use in stratospheric modeling
37. Wang L, Liu JY, Li ZS, Huang XR, Sun CC (2003) J Phys Chem A 107:4921
38. Li B, Liu JY, Li ZS, Wu JY, Sun CC (2004) J Chem Phys 120:6019
39. Xiao JF, Li ZS, Liu JY, Li S, Sun CC (2003) J Phys Chem A 107:267
40. Xiao JF, Li ZS, Ding YH, Huang XR, Sun CC (2002) J Mol Struct 582:53
41. Xiao JF, Li ZS, Ding YH, Liu JY, Huang XR, Sun CC (2002) J Phys Chem A 106:320